Central Region Technical Attachment
Number 13-02
July 2013

Analysis of the 26 August 2007 Northern Plains Tornado Outbreak

Chauncy J. Schultz
National Weather Service
Billings, Montana

David J. Kellenbenz and James W. Kaiser
National Weather Service
Grand Forks, North Dakota

ABSTRACT

Eleven tornadoes struck North Dakota and Minnesota as part of a regional, late-season outbreak on 26 August 2007. Large convective available potential energy (CAPE) values were present amidst moderate deep-layer vertical wind shear. An expectation for strong capping and slightly veered surface winds made anticipating convective initiation and tornado potential difficult early in the event. However, once discrete supercell thunderstorms matured, conditions became favorable for tornadogenesis. An EF4 tornado struck Northwood, North Dakota following the merger of two supercells. The Northwood tornado occurred within 30 km of the nearest WSR-88D radar (KMVX at Mayville, North Dakota). This study will investigate the synoptic and mesoscale setting of this tornado event and the close-range radar observations of the violent Northwood tornado.

---

1. Introduction

Discrete supercells produced eleven tornadoes in North Dakota and Minnesota on 26 August 2007, including one EF2, one EF3, and an EF4 (on the Enhanced Fujita [EF] scale) that struck Northwood, North Dakota (population approximately 1,000) at 0145 UTC 27 August 2007 (Figs. 1 and 2). Nine of the tornadoes were in North Dakota, totaling around 40% of the state's annual average. The Northwood tornado was estimated to be 1.3 km (0.8 miles) wide at its maximum, and caused one fatality (the first in North Dakota since 1997), eighteen injuries, and property damage totaling more than $52 million (Fig. 3). Strong tornadoes are a relatively rare occurrence in North Dakota during the late summer period. In fact, approximately 45% of

all EF3-EF5 tornadoes in the region take place between 15 June and 15 July per the National Oceanic and Atmospheric Administration's (NOAA) *Storm Data* publication (Fig 4).

The convective available potential energy (CAPE) and wind shear present on 26 August 2007 were consistent with the empirical results derived from many historical strong and violent tornadoes (e.g., Rasmussen and Blanchard 1998 and Thompson et al. 2003). However, the presence of a strong capping inversion associated with the elevated mixing layer (EML) and slightly veered boundary layer winds led to reduced confidence in the potential for a tornado outbreak in this case. These issues will be discussed along with the synoptic and mesoscale environments in section 2 of this paper.

The Northwood tornado occurred approximately 30 km from the Mayville, North Dakota WSR-88D (KMVX). The close-proximity weather radar observations of the EF4 tornado will be investigated in section 3. Section 4 will summarize the findings of this paper.

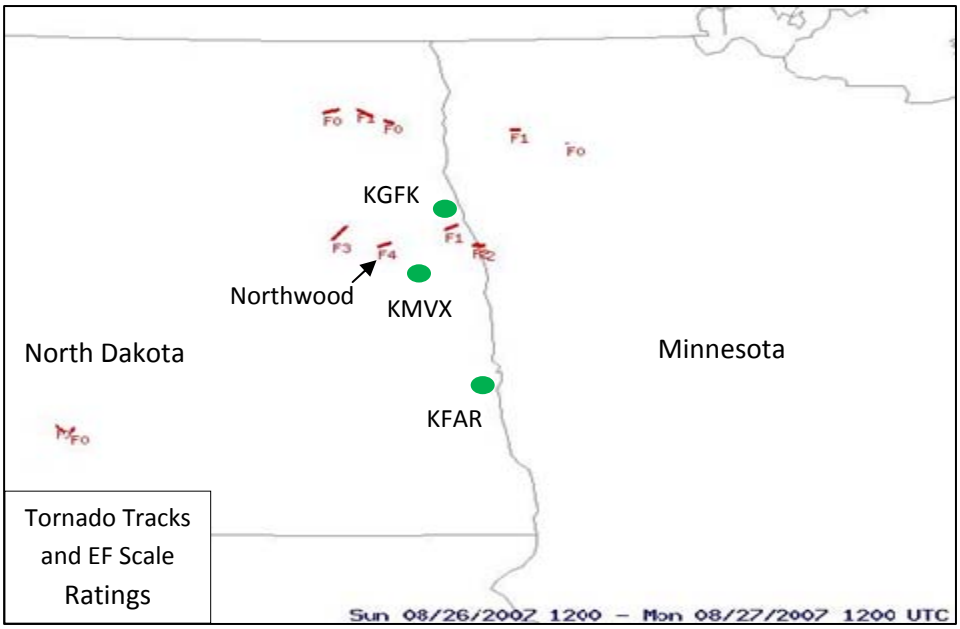

Figure 1. Documented tornado tracks and EF-scale ratings over North Dakota and northwestern Minnesota on 26 August 2007. Locations of the Mayville, North Dakota WSR-88D (KMVX) and the nearest large cities (Grand Forks, North Dakota [KGFK], and Fargo, North Dakota [KFAR]) are also annotated.

Figure 2. Photograph showing the rain-wrapped Northwood, North Dakota tornado at 0155 UTC 27 August 2007, minutes after striking the community (credit: Aaron Kennedy; used with permission).

Figure 3. Photographs taken by a National Weather Service storm survey team, showing tornado damage up to EF4 intensity in Northwood, North Dakota.

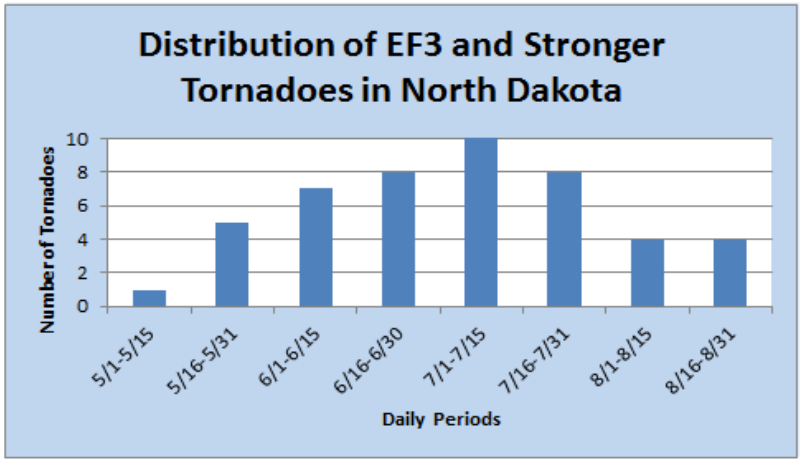

Figure 4. Histogram of daily periods when tornadoes of EF3 and greater intensity have been recorded in North Dakota from 1950 to 2012 (from NOAA *Storm Data*). Note that the tornadoes from 26 August 2007 have been included in this histogram.

2. Environmental Conditions and Forecast Implications

a. Synoptic and mesoscale setting

Nearly zonal mid- and upper-level flow preceded the tornado outbreak. The 1200 UTC 26 August 2007 upper-air observations revealed a 75 kt 250-hPa jet along the United States-Canadian border in central Montana. This jet segment moved east-northeastward during the day, and was just northwest of the tornado outbreak area by 0000 UTC 27 August 2007 (Fig. 5). The fact that the jet streak was slightly displaced from the area affirms the subtle nature of the event, especially since the region was in the right exit region of the jet, where downward motion is implied aloft (Bluestein 1993). However, the outbreak's location near the right exit region of the upper jet streak was actually consistent with the results of Rose et al. (2004), which found both exit regions to be favored locations for strong tornadoes.

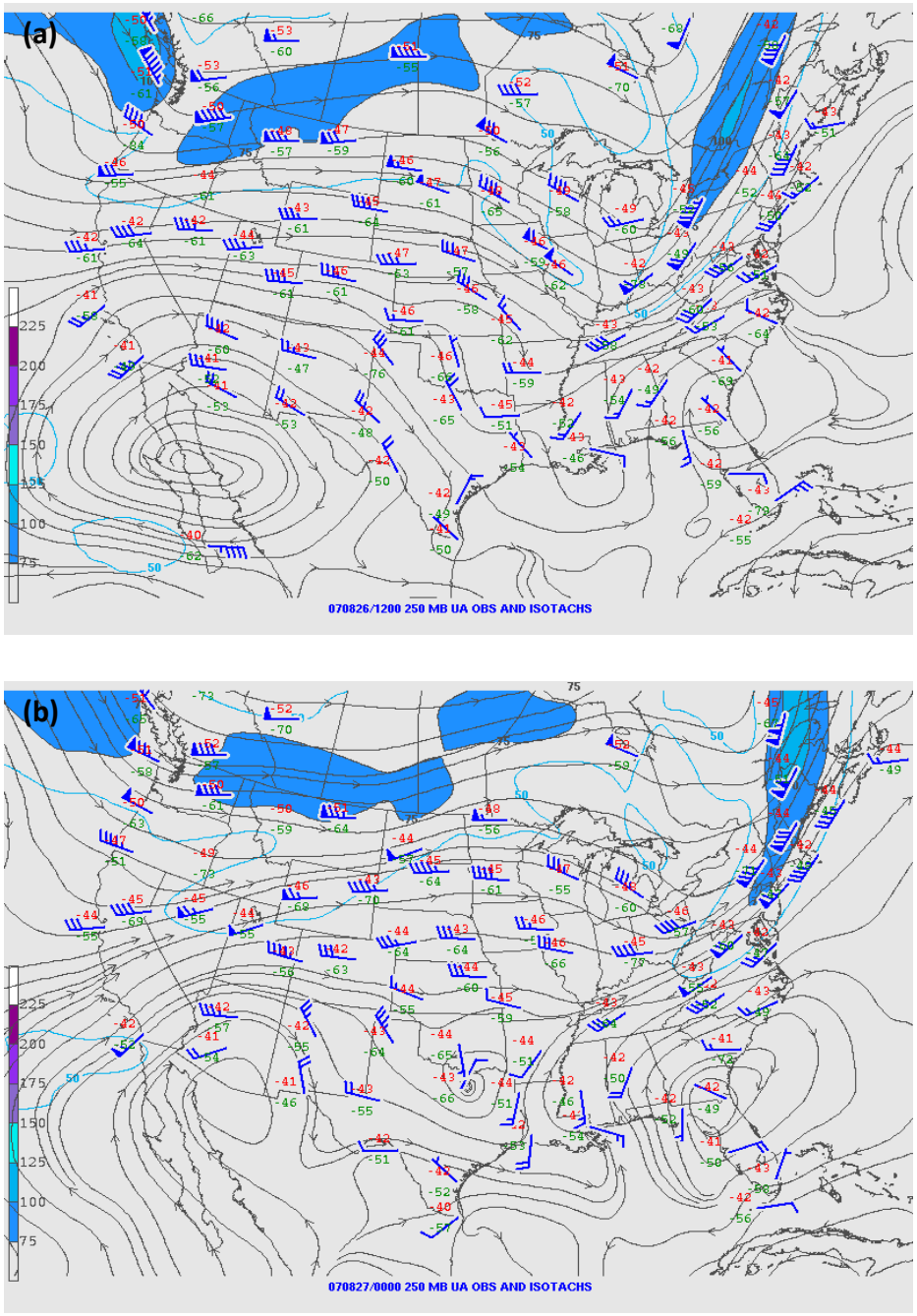

Figure 5. Storm Prediction Center (SPC) 250-hPa analysis with station observations in conventional form, streamlines, and isotachs (colored, contour interval = 25 kt) at a) 1200 UTC 26 August 2007 and b) 0000 UTC 27 August 2007.

A surface pressure trough, which served as the focus for tornadic supercells on 26 August 2007, moved from west-central North Dakota at 1800 UTC to east-central and northeastern North Dakota by 0000 UTC (Figs. 6 and 7). The trough extended from a surface low pressure system that was located in southeastern Manitoba by early evening. The forecast was complicated by the outbreak's location along a surface trough, since Johns et al. (2000) showed the region's favored location for significant tornadoes to be in the northeastern quadrant of a surface low pressure system.

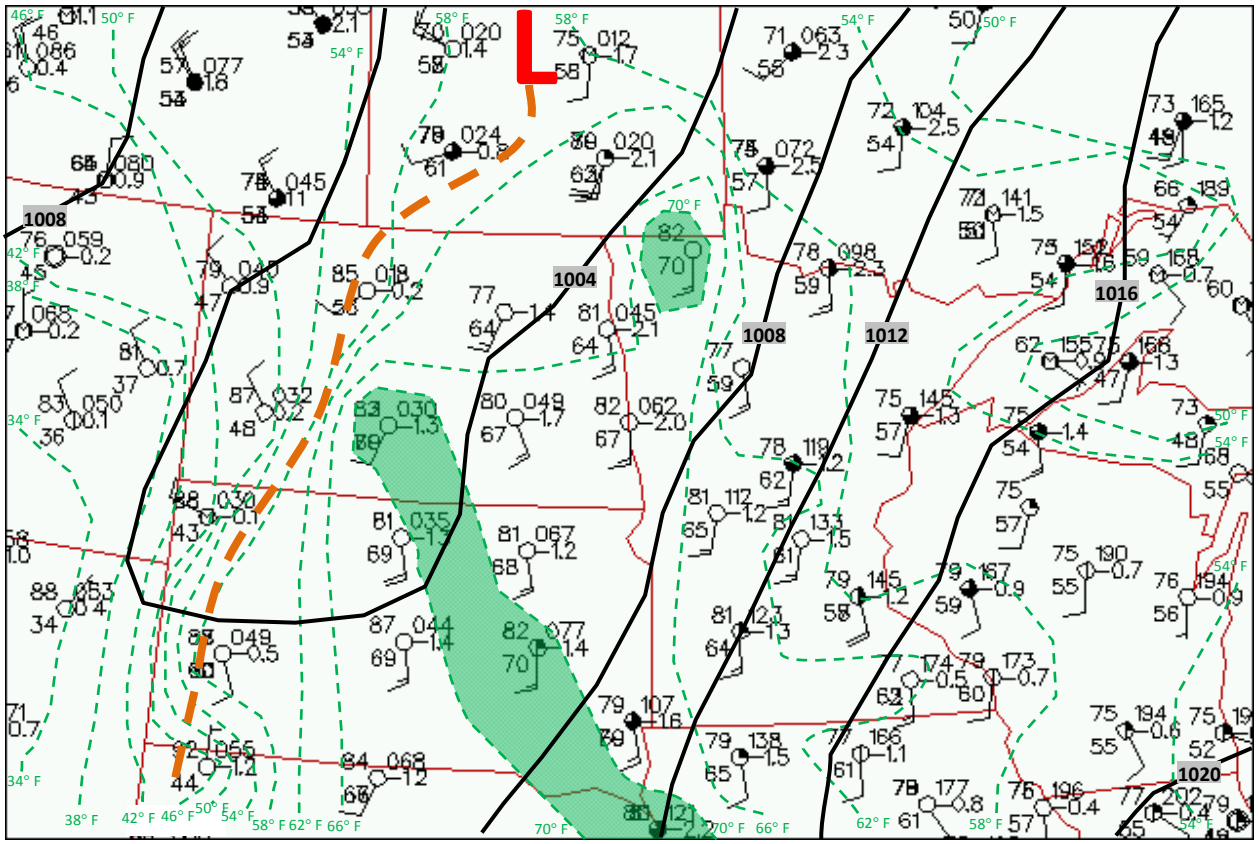

Figure 6. Surface map at 1800 UTC 26 August 2007 with conventional surface observations, isobars (solid black contours, contour interval = 4 hPa), and isodrosotherms (green dashed contours, contour interval = 4° F, with values ≥ 70° F shaded solid green).

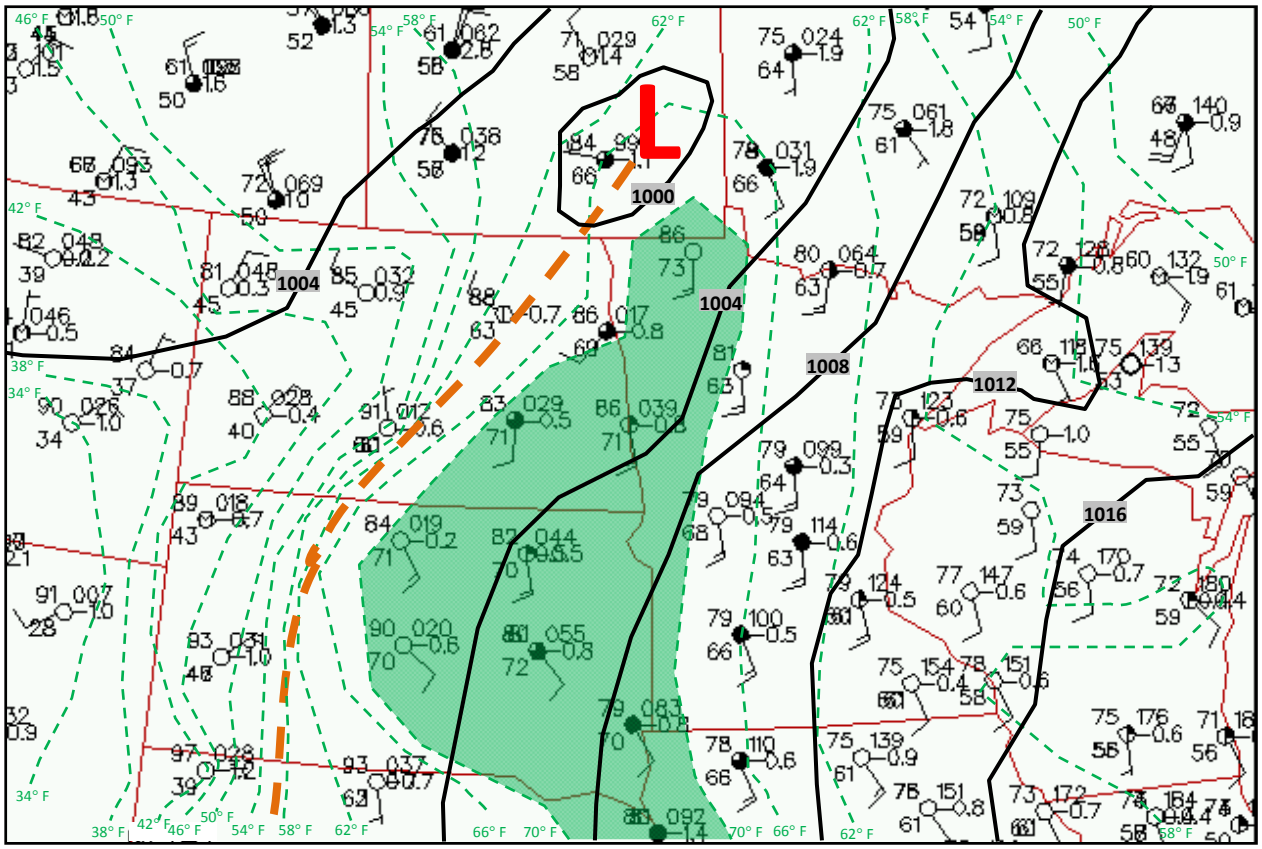

Figure 7. As in Fig. 6, but for 0000 UTC 27 August 2007.

Strong low-level moisture advection occurred across the region on 26 August 2007. Surface dew points increased from 7-10° C (45-50° F) at 1200 UTC to 18-23° C (65-73° F) by 0000 UTC. A notable EML was also transported eastward across the Plains on increasing westerly flow aloft, which caused the 700–500-hPa temperature lapse rates to exceed 7° C km^{-1} in this region (not shown). This contributed to large CAPE, but also led to significant capping. Meanwhile, west of the surface trough, solar insolation caused surface temperatures to rise near 32° C (90° F) within a well-mixed boundary layer. The moisture gradient across the boundary was relatively weak; surface dew points remained near 15° C (59° F) just behind the westerly wind shift. However, the vertical extent of boundary layer moisture was considerably less in the

wake of the trough, as shown by the comparison between 0000 UTC soundings from Bismarck, North Dakota (KBIS) and Aberdeen, South Dakota (KABR) in Fig. 8.

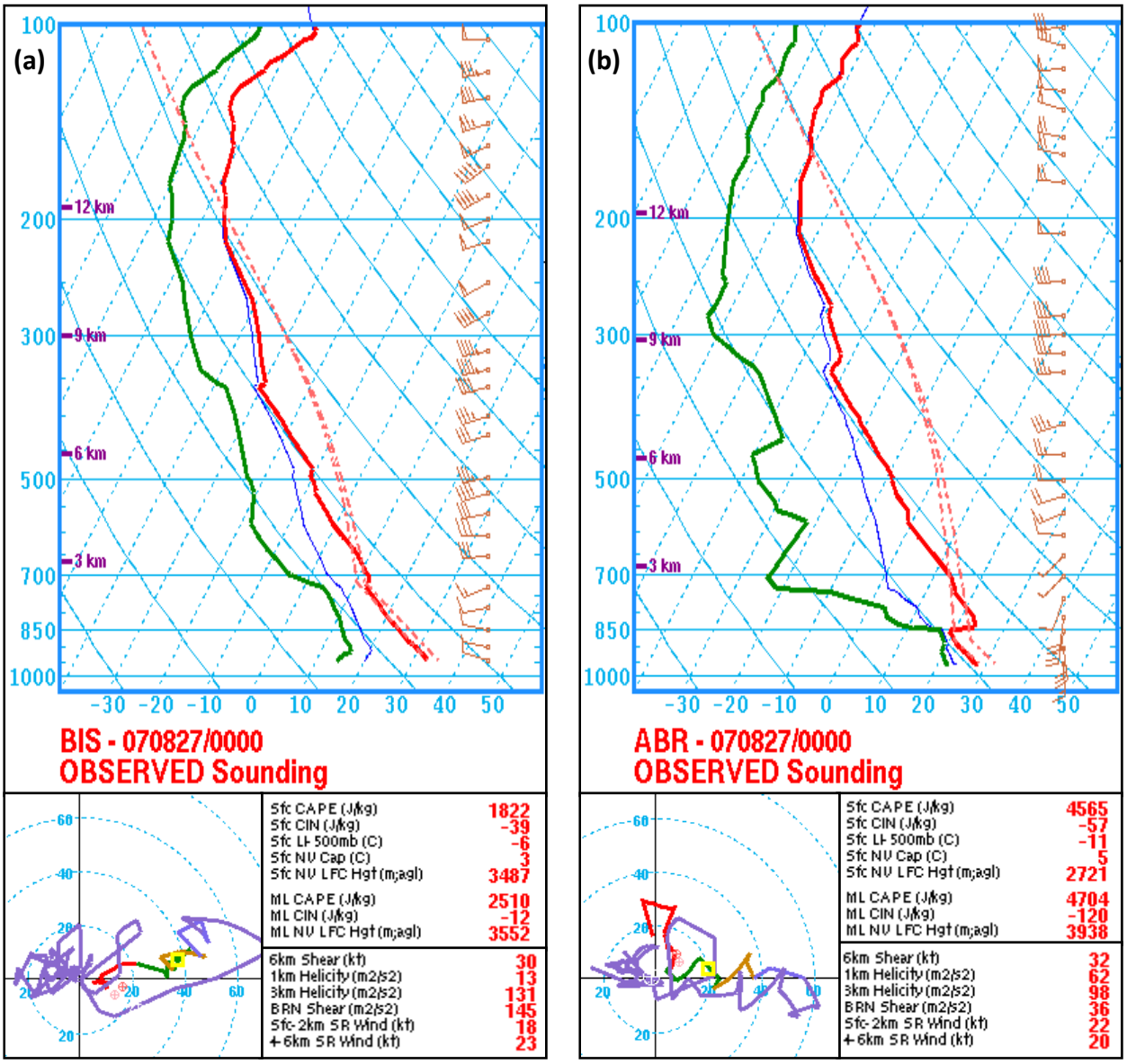

Figure 8. Skew T diagrams, hodographs, and calculated parameters of the 0000 UTC 27 August 2007 soundings from a) KBIS and b) KABR.

The substantial low-level moisture and relatively uninhibited surface heating east of the trough led to large instability. The 0000 UTC KABR sounding in Fig. 8b sampled around 4500 J kg^{-1} of both surface-based CAPE (SBCAPE) and 100-hPa-mean layer CAPE (MLCAPE). In addition, Rapid Update Cycle (RUC) objective analyses suggested that the axis of MLCAPE values of at least 3000 J kg^{-1} extended into northeastern North Dakota by 0000 UTC (Fig. 9). Although CAPE alone has not been shown to be particularly useful in discriminating between tornadic and non-tornadic supercells (e.g., Rasmussen and Blanchard 1998), high-end values have been noted in close proximity to other strong and violent tornadoes, such as the Greensburg, Kansas EF5 event of 4 May 2007 (Lemon and Umscheid 2008). Thompson et al. (2003), in their RUC-based study, also found significant tornado cases to have higher median MLCAPE (2152 J kg^{-1}) than weak tornadoes (1835 J kg^{-1}).

RUC analyses, such as the one from 2000 UTC in Fig. 9a, suggested -50 to -100 J kg^{-1} of 100-hPa-mean layer convective inhibition (MLCIN) was present ahead of the surface trough in eastern North Dakota during the afternoon, but that weakened considerably by 0000 UTC (Fig. 9b). Convective initiation occurred between 2230 and 2330 UTC. However, most model simulations leading up to the event maintained significant capping along the surface trough, and produced minimal convective precipitation south of the Canadian-United States border. One exception to the dry forecasts was the high-resolution, convection-resolving Non-hydrostatic Mesoscale Model version of the Weather Research and Forecasting model (WRF-NMM) generated by the National Center for Environmental Prediction (NCEP) 24 hours prior to the outbreak (not shown). However, that simulation alone was not enough to enhance marginal confidence in a spatially significant severe weather episode. This, in turn, leads to the following

questions: "*What processes were in place to sufficiently weaken the cap for convective initiation, and could this have been anticipated from observed or model data?*"

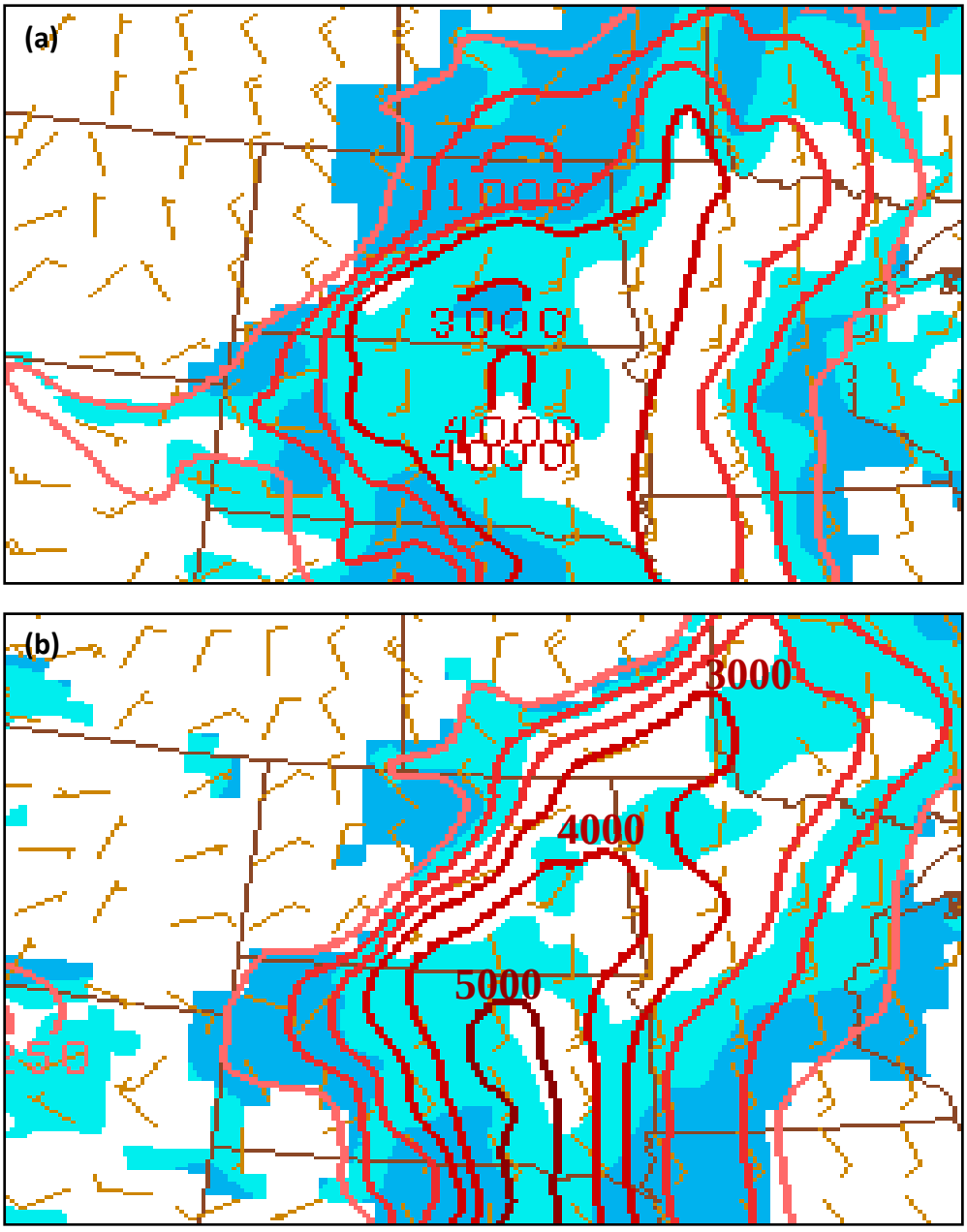

Figure 9. RUC 00-hour analysis of MLCAPE (red contour) and MLCIN (light blue shaded area = -50 J kg^{-1} and darker blue shaded area = -100 J kg^{-1}) at a) 2000 UTC 26 August 2007 and b) 0000 UTC 27 August 2007.

Garner (2008) stated that one ideal setting for intense convective development occurs when an upper-level disturbance approaches a region of well-mixed boundary layer air characterized by steep 0–3-km temperature lapse rates that extend into a downstream region containing rich, deep low-level moisture, potentially identified by the overlap of steep 0–3-km temperature lapse rates and MLCAPE. Figure 10 shows the RUC analysis of these two fields at 2300 UTC 26 August 2007, near the time of convective initiation. A narrow ribbon of overlap between steep 0–3-km temperature lapse rates (greater than 8° C km^{-1} in this case) and 0–3-km MLCAPE (greater than 75 J kg^{-1} in this case) is evident, almost perfectly in line with the zone of convective initiation. Similar overlap has been observed prior to other strong tornadoes in the northern Plains (e.g., Kellenbenz et al. 2007 and Schultz 2009). These observations lend credence to the hypothesis that the intense supercells in the 26 August 2007 case developed at the interface of a hot, relatively dry, deeply-mixed boundary layer air mass and a strongly unstable, but capped one.

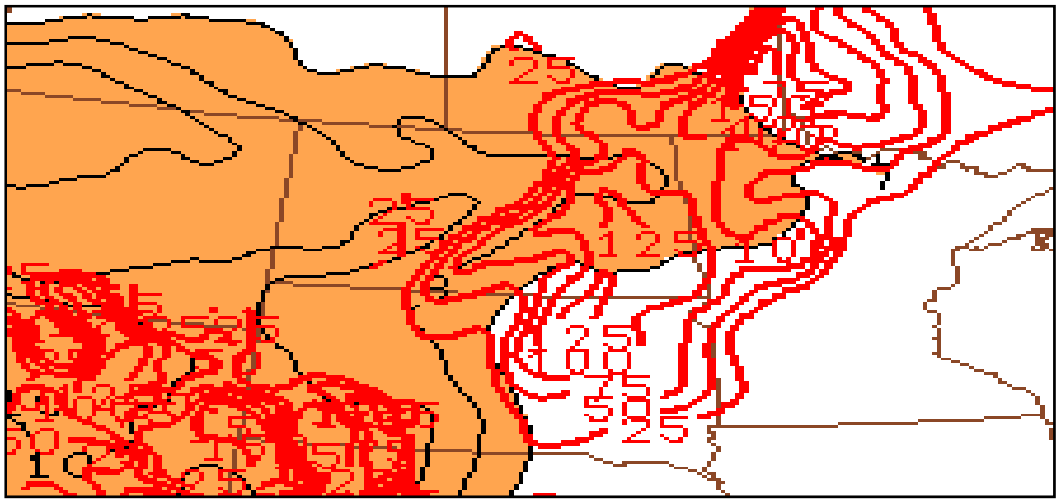

Figure 10. RUC analysis of 0–3-km temperature lapse rate (solid black contours, CI = 1°C km^{-1} for values beginning at 7°C km^{-1}, which is denoted by solid orange shading) and 0–3-km MLCAPE (solid red contours, contour interval = 25 J kg^{-1}) at 2300 UTC 26 August 2007.

The series of satellite images in Fig. 11 also suggest that high-based cumulus (observed bases > 1500 m above ground level [AGL]) may have initially developed in the hot, relatively dry, but well-mixed boundary layer air mass, and then intensified upon moving downstream into the more unstable air mass. By 0003 UTC, mature supercells had formed along and east of the surface trough (Fig. 12). This evolution toward a significant tornado outbreak, rather than a cap-inhibited "non-event," was subtle at best. Model data alone likely would not have made forecasters anticipate a break of the cap. This is because forecast soundings, even along the surface trough, displayed large convective inhibition through the entire diurnal heating cycle. Only careful scrutiny of observational data and objective analysis products in the period leading up to convective initiation could account for those shortcomings.

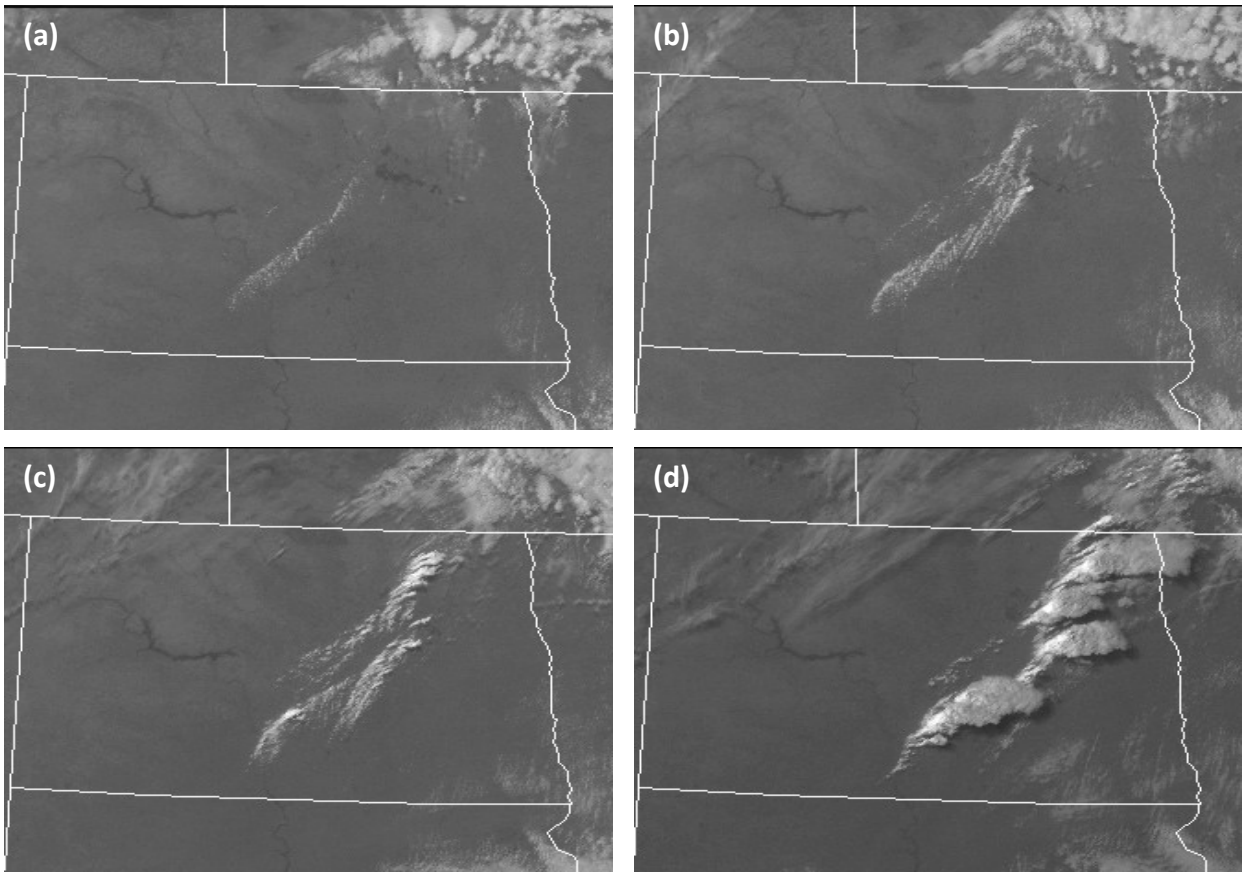

Figure 11. GOES-12 visible satellite imagery series on 26 August 2007 at a) 2045 UTC b) 2130 UTC c) 2215 UTC and d) 2315 UTC.

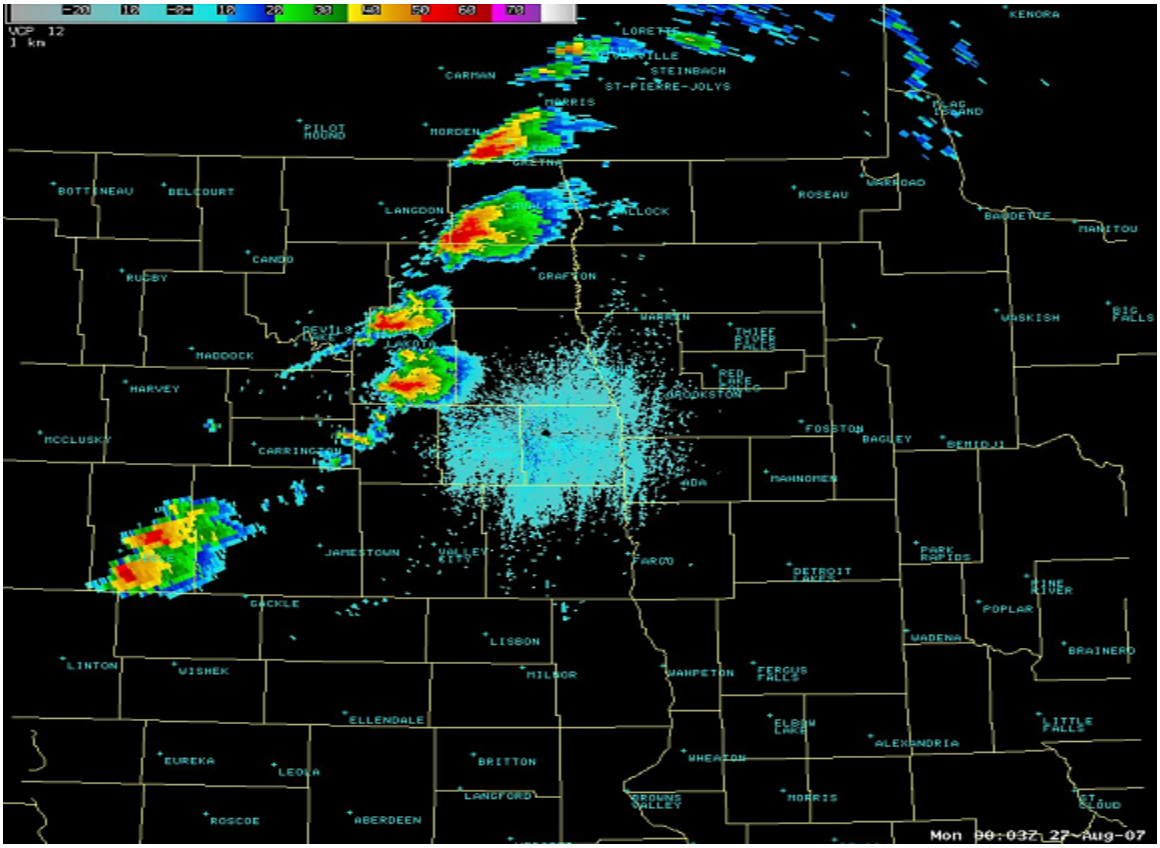

Figure 12. KMVX WSR-88D 0.5° radar reflectivity imagery at 0003 UTC 27 August 2007.

b. Vertical wind shear, storm-relative helicity (SRH), and storm-relative (SR) winds

Strengthening mid- and upper-level wind fields contributed to bulk vertical wind shear sufficient for supercellular convection by 0000 UTC 27 August 2007. The 0–6-km bulk wind shear vector magnitude was in excess of 30 kt over the region, while 0–8-km bulk wind shear vectors approached 50 kt. The results of Bunkers et al. (2006b) suggest that this magnitude of shear was indeed sufficient for supercells. Although the degree of CAPE and vertical wind shear made anticipation of a supercellular convective mode relatively straightforward, the tornado

forecast was complicated to some extent by the surface wind direction containing a slightly southwesterly component in northeastern North Dakota, as shown in Fig. 7.

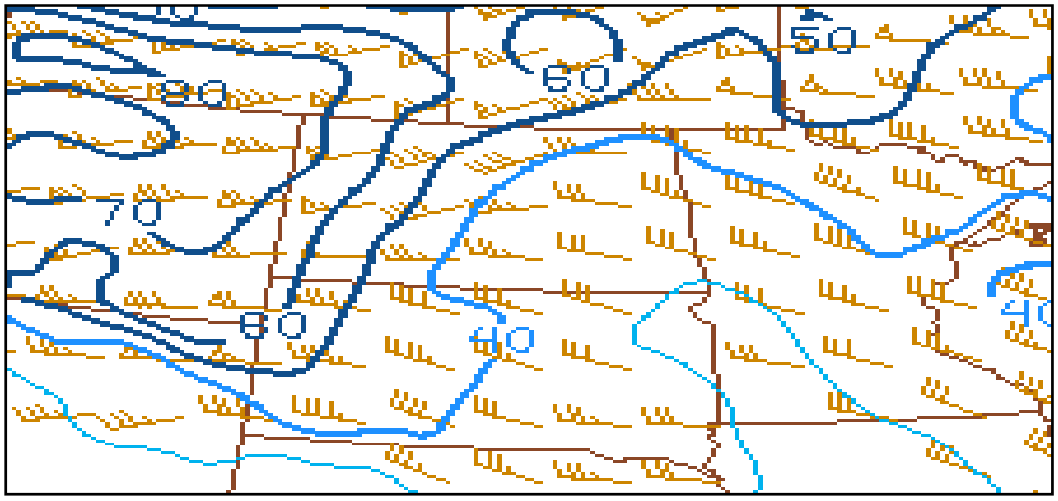

Figure 13. RUC 00-hour analysis of 0–6-km bulk wind shear vectors and magnitude (solid blue contours, CI = 10 kt beginning at 30 kt) at 0000 UTC 27 August 2007.

Despite the lack of an easterly component to the surface winds, approximately 20 kt of 0–1-km bulk wind shear was present in far eastern North Dakota and all of northwestern Minnesota after 0000 UTC. This is near the median value of 0–1-km bulk wind shear associated with strong tornado cases in Thompson et al. (2003). This was confirmed by hodographs constructed using the velocity azimuth display (VAD) wind profile from KMVX (Fig. 14). The hodographs display strong speed shear in the lowest 1 km, and strong directional shear above. This resulted in a "sickle" shape to the hodographs similar to those associated with several strong and violent tornado events (Miller 2006), even if their size was not as large as more prominent cases. Given average supercell propagation motions from 270° in this case, the *storm-relative* wind shear was similar to northeastward-moving supercells in an environment characterized by easterly surface

winds. RUC objective analyses[1] suggested that 0-1-km storm-relative helicity (SRH) was over 150 m^2 s^{-2}. However, applying the observed storm motion of the Northwood supercell at the time of its violent tornado (270° at 13 m s^{-1}) to the time-series of hodographs derived from the VAD wind profile (VWP) in Fig. 14 reveals that 0–1-km SRH actually increased to around 200 m^2 s^{-2} by 0045 UTC. These values are again very near the median of significant tornado cases in the Thompson et al. (2003) empirical study. Moreover, Kerr and Darkow (1996) found a mean 0–1-km SRH of 186 m^2 s^{-2} for the F4 tornadoes in their sample.

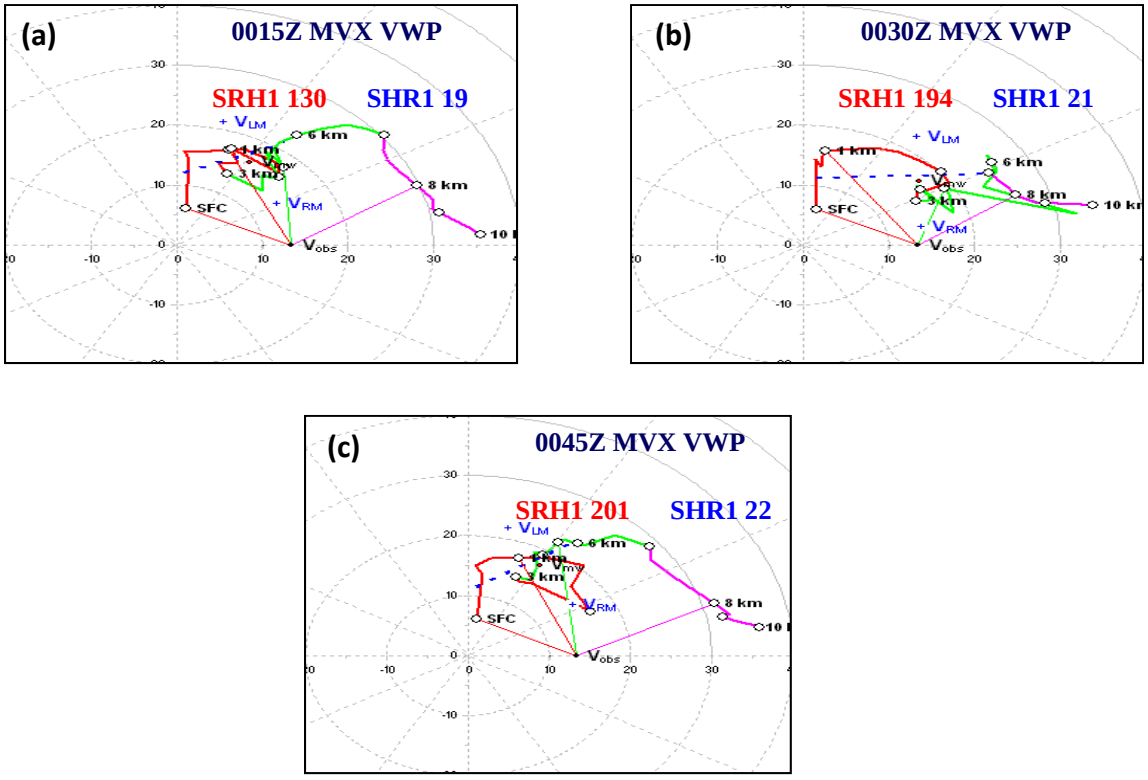

Figure 14. Hodographs derived from the KMVX velocity azimuth display (VAD) wind profile and fit to 250-m input levels on 27 August 2007 at a) 0015 UTC b) 0030 UTC and c) 0045 UTC. The left-moving (LM) and right-moving (RM) cell propagation suggested by the internal dynamics (ID) method (Bunkers et al. 2000) are also annotated. Storm-relative calculations used an observed motion of 270° at 13 m s^{-1}.

[1] RUC objective analyses of storm-relative helicity and storm-relative winds discussed in this paper rely on the internal dynamics method of supercell motion developed by Bunkers et al. (2000).

Storm-relative winds were also notable during the tornado outbreak. The 0–2-km storm-relative winds from objectively analyzed RUC data were around 25 kt at 0000 UTC (Fig. 15). Similar magnitudes of 0–2-km storm-relative winds to those objectively analyzed near Northwood, North Dakota were also noted with objectively analyzed RUC data near the Greensburg, Kansas EF5 tornado on 4 May 2007 (not shown), and the Barnes County, North Dakota F4 tornado event on 18 July 2004 (Kellenbenz et al. 2007).

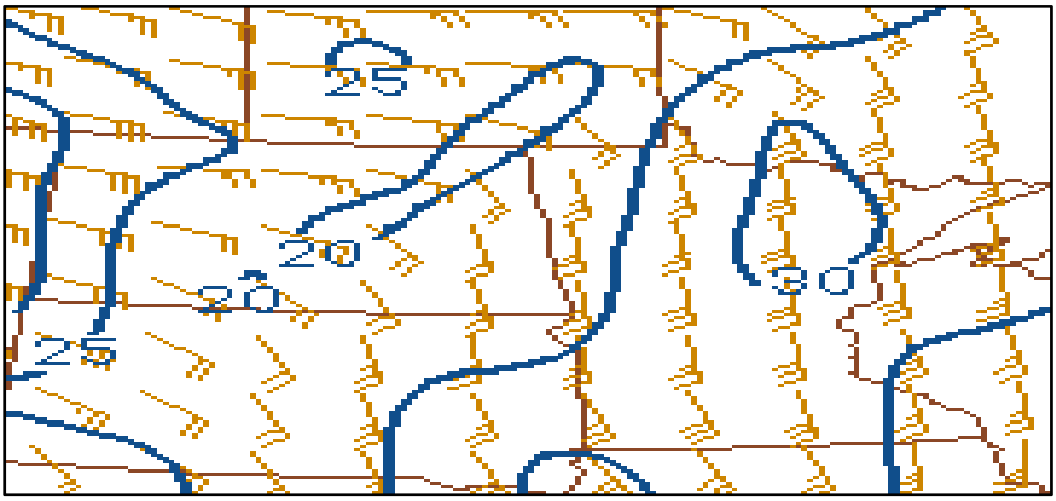

Figure 15. RUC 00-hour analysis of 0–2-km storm-relative wind vectors and magnitude (solid blue contours, contour interval = 5 kt beginning at 20 kt) at 0000 UTC 27 August 2007.

Storm-relative winds veered from southerly in the 0–2-km layer to a westerly direction aloft. Anvil-level storm-relative winds backed from a west-southwest to a westerly direction during the afternoon, and increased from 40 kt at 1800 UTC (not shown) to at 55 kt at 0000 (Fig. 16). Increasing storm-relative winds with height likely allowed hydrometeors to be carried away from the supercell updrafts, which can allow mesocyclones to persist for longer periods of time (Brooks et al. 1994). Interestingly, mid-level storm-relative winds in the 4–6-km layer backed from the west to the southwest during the afternoon, and decreased from 25 kt at 1800 UTC to

around 15 kt at 0000 UTC (not shown). However, the speeds by 0000 UTC were still near the range favorable for significant supercell tornadoes based on Thompson et al. (2003).

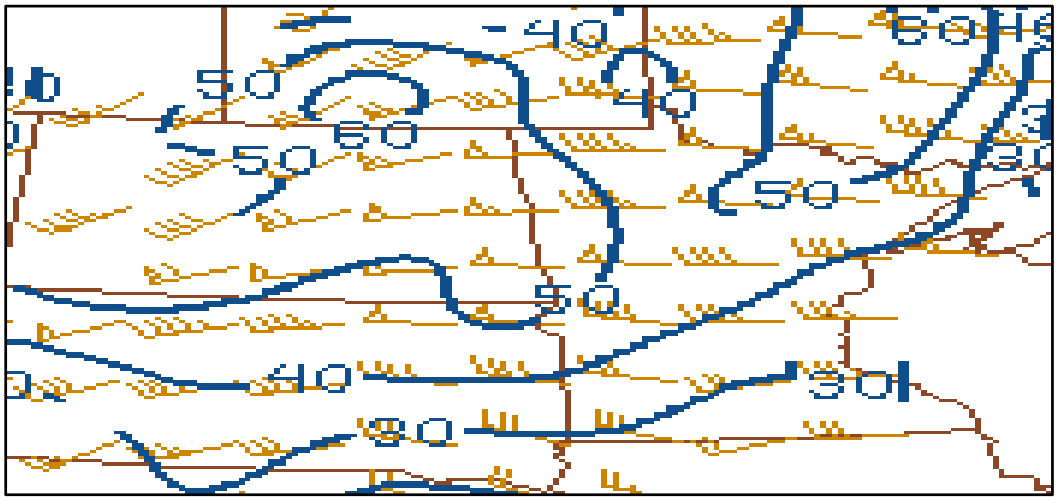

Figure 16. RUC 00-hour analysis anvil-level storm-relative wind vectors and magnitude (solid blue contours, contour interval = 10 kt beginning at 30 kt) at 0000 UTC 27 August 2007.

c. CAPE-shear environment

Both the CAPE and shear values on 26 August 2007 fell within the range of previously observed significant tornado events. However, given the question of tornado threat leading up to supercell initiation, it is important to quantify the CAPE-shear *combination* in the context of other historical, significant tornado events. One way to do this is through the 0–1-km energy helicity index (EHI; Hart and Korotky 1991). The 0–1-km EHI on 26 August 2007 exceeded 3 over the entire outbreak area, and was 4 in the vicinity of Northwood, as demonstrated by the 0100 UTC RUC interpolated sounding for Grand Forks, North Dakota (41 km northeast of Northwood) shown in Fig. 17. To place this into perspective, the 90th percentile 0–1-km EHI of significant tornado cases in Rasmussen (2003) was only 1.99. Another late-season (26 October

1996), high-shear tornado outbreak across the northern Plains with comparable EHI values was described in Bramer et al. (1998).

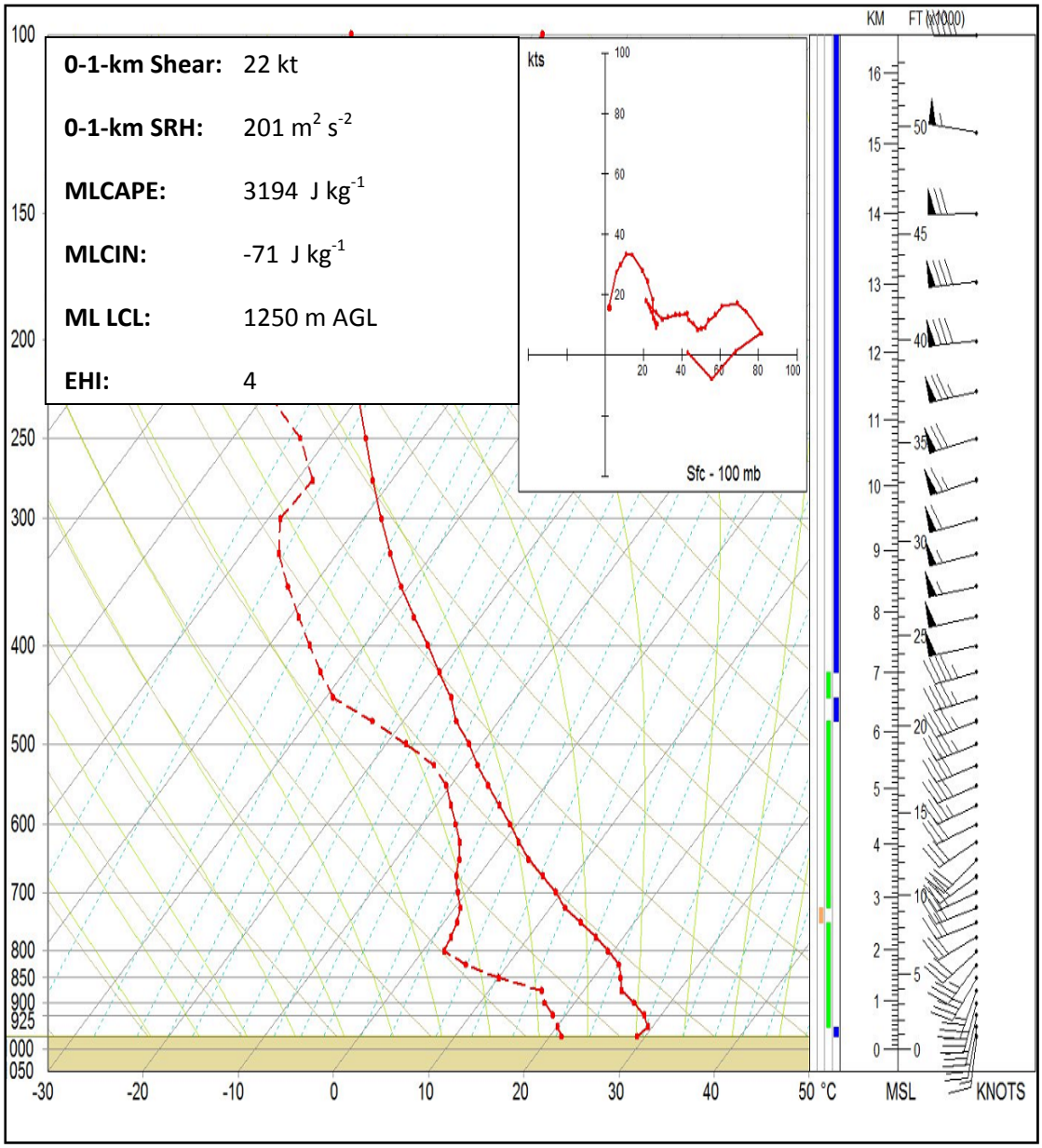

Figure 17. Skew T diagram, hodograph, and calculated parameters from the RUC 00-hour analysis sounding at Grand Forks, North Dakota at 0100 UTC 27 August 2007.

The RUC-based soundings taken in the outbreak area were also comparable analogs to several other tornado events, and distinctly reminiscent to a late-spring, southern Plains tornado episode (R. L. Thompson 2007, personal communication). Despite a somewhat atypical surface pattern, the overall environment was primed for significant tornadoes, given initiation of deep, moist convection in the initially capped environment.

The RUC sounding in Fig. 17 also suggests that the nocturnal radiation inversion may have already been developing by the time of the violent Northwood tornado, contributing in part to the -72 J kg^{-1} of MLCIN shown. Davies and Fischer (2009) found that mesocyclones may be strong enough to overcome low-level stability associated with boundary layer cooling when unusually large CAPE values exist in the first few hours after sunset. On 26 August 2007, supercells which were already mature at sunset likely maintained themselves in a high-end CAPE-shear setting for a short period after dark.

In order to make a more direct comparison of the Northwood tornado environment to other significant late-season tornadoes, a combination of RUC objective analysis and observed sounding data was collected for twenty-six F/EF2 and stronger tornadoes which occurred in the north-central United States between August 1st and October 31st. The tornadoes are listed in Table 1. Multiple events from the same day were used if the tornadoes were separate and occurred in a different analysis hour. Values of 0–1-km bulk wind shear, 0–1-km SRH, MLCAPE, MLCIN, and 100-hPa-mean layer lifted condensation level (MLLCL) height were retrieved for each tornado, and a comparison of median parameter values from that data set and the Northwood estimated environment is shown in Table 2. In general, the Northwood tornado occurred with very similar low-level shear as other significant late-season tornadoes in the north-

central United States. However, the Northwood tornado occurred in an environment with much larger MLCAPE than similar late-season events.

TABLE 1. List of significant, late-season tornadoes (F/EF2 and stronger tornadoes that occurred between August 1st and October 31st) from the north-central United States.

Date	Location	Strength	Analysis Time (UTC)	Analysis Type
8/18/1968	Southeast NE	F3	00	Sounding
9/1/1973	Southeast MN	F2	00	Sounding
8/26/1977	Central MN	F3	00	Sounding
9/3/1980	Central MN	F3	00	Sounding
10/26/1996	Central MN	F2	00	Sounding
8/18/2005	Southwest WI	F2	21	RUC
8/18/2005	Southwest WI	F2	22	RUC
8/18/2005	South-central WI	F3	23	RUC
9/5/2005	Southeast ND	F2	01	RUC
9/21/2005	Southeast MN	F2	00	RUC
8/1/2006	Southwest MN	F3	00	RUC
8/5/2006	Northwest MN	F3	00	RUC
8/24/2006	Central ND	F2	19	RUC
8/24/2006	South-central MN	F3	22	RUC
8/24/2006	North-central SD	F3	22	RUC
8/24/2006	East-central SD	F3	23	RUC
8/24/2006	East-central SD	F2	00	RUC
9/15/2006	Southeast NE	F2	01	RUC
9/16/2006	Southeast SD	F2	21	RUC
9/16/2006	Southeast MN	F2	03	RUC
9/30/2007	Central IA	EF2	23	RUC
8/7/2010	West-central MN	EF4	23	RUC
8/10/2010	Northeast ND	EF2	18	RUC
8/12/2010	Northwest ND	EF3	02	RUC
8/11/2011	North-central NE	EF3	01	RUC
8/23/2011	Central WI	EF2	22	RUC

TABLE 2. Comparison of median parameter values for twenty-six significant, late-season tornadoes in the north-central United States and the environment near Northwood, North Dakota on 26 August 2007 estimated from RUC analyses and VWP data.

Parameter	**Median value for 26 significant, late-season tornadoes in the north-central United States**	**Estimated Northwood, North Dakota parameter value**
0-1-km bulk wind shear magnitude	23 kt	22 kt
0-1-km SRH	233 $m^2 s^{-2}$	201 $m^2 s^{-2}$
ML LCL Height	1071 m AGL	1250 m AGL
MLCAPE	1936 J kg^{-1}	3194 J kg^{-1}
MLCIN	-24 J kg^{-1}	-71 J kg^{-1}

d. Maintenance of discrete supercells

Although the CAPE-shear setting in this case initially supported discrete supercells, it was not entirely clear whether or not the supercells would remain discrete, or even whether or not upscale growth into a linear convective complex would occur. The question of discrete supercell maintenance in this event arose primarily as a result of high-resolution numerical model results. The 4-km WRF NMM and National Severe Storms Laboratory (NSSL) WRF reflectivity forecasts from 0000 UTC 26 August 2007 (nearly 24 hours prior to the tornado outbreak) suggested that the primary convective mode would become linear relatively quickly after convective initiation (R. L. Thompson 2007, personal communication). A linear convective mode generally reduces the threat of significant tornadoes (Thompson and Mead 2006). Even though the high-resolution models suggested a linear convective mode, there were at least two

prominent environmental conditions negating its occurrence. The first was the nearly normal orientation of the deep-layer shear vectors to the primary low-level lifting mechanism (i.e., the surface trough). Dial and Racy (2004) found that, when the mean 2-8-km flow was more perpendicular to a boundary, precipitation was less likely to cascade among cells, and outflows of neighboring cells consolidated more slowly, both of which maintained discrete cells longer. The second condition supporting maintenance of discrete convection on 26 August 2007 was forcing along a surface trough, rather than a cold front. That is because initiation along surface troughs tends to produce discrete modes more readily than initiation along cold fronts (Dial and Racy 2004).

Although a case has been made for the supporting nature of the low-level shear (and SRH) present on 26 August 2007, it must be noted that the magnitude of near-surface shear increased during the evening, and with eastward extent from the surface trough. Locations immediately along the surface trough at 2200 UTC (when convection initiated) only experienced 15 kt of 0–1-km bulk wind shear. Only after 0000 UTC, and about 110 km east of the initiation zone, were the previously described strong shear profiles present. Even though a low-level jet did not strengthen during that time, surface winds did decrease, thus increasing low-level speed shear. Moreover, the height of the lifted condensation level (LCL) decreased with time and eastward extent, as well, dropping to around 1200 m AGL after 0000 UTC (from approximately 1500 m AGL at 2200 UTC). Thus, in order to maximize tornado potential, discrete supercell maintenance was necessary for at least 2 to 3 hours. This is easily reflected in the tornado reports; none occurred until after 0000 UTC, even though some storms produced severe hail before that time.

3. Close-proximity WSR-88D observations of the Northwood tornado

Few strong or violent tornadoes have been sampled in close proximity (≤ 60 km) to a WSR-88D. Notable exceptions include the F5 Moore, Oklahoma tornado on 3 May 1999 and the EF5 tornado at Greensburg, Kansas on 4 May 2007 (Burgess et al. 2002 and Lemon and Umscheid 2008, respectively), as well as the EF5 tornadoes at Moore, Oklahoma on 20 May 2013 and near El Reno, Oklahoma on 31 May 2013. The Northwood, North Dakota EF4 tornado occurred only 30 km from the KMVX WSR-88D, with 0.5° elevation data only 217 m (888 feet) AGL, so KMVX also offered notable close-range views of a violent tornado cyclone circulation.

The rapid increase in low-level gate-to-gate (GTG) shear and subsequent Northwood tornadogenesis occurred following a merger between a cyclonically rotating supercell that produced an earlier EF3 tornado about 28 km west of Northwood (called supercell A), and the cyclonically rotating supercell that approached Northwood from the west-southwest called supercell B). Figure 18 shows both supercells and their respective storm motions at 0054 UTC.

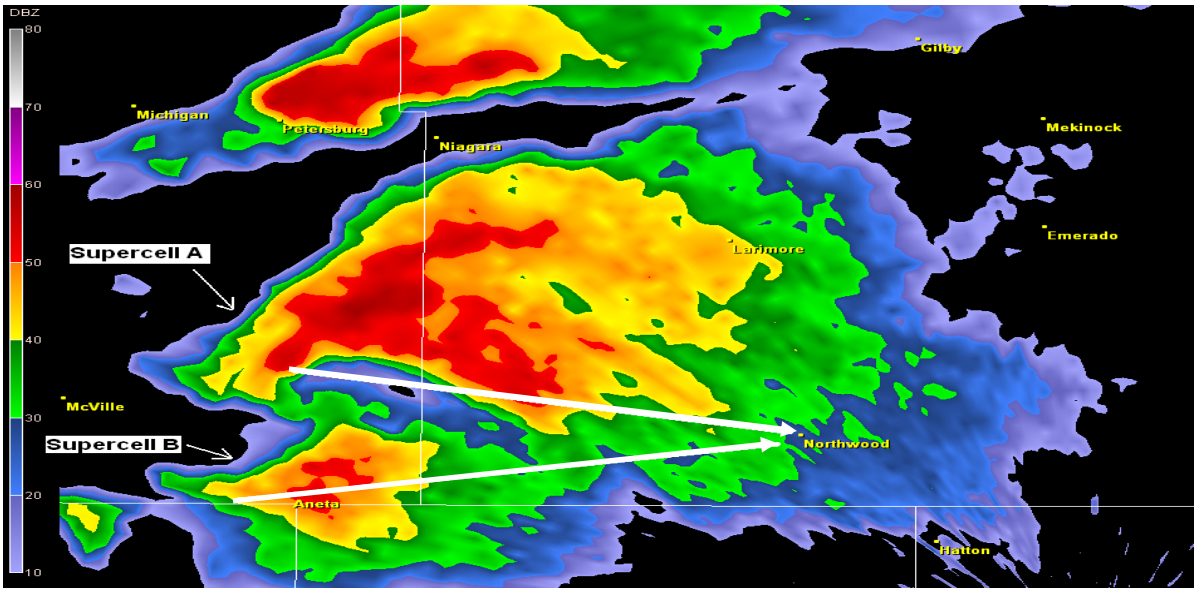

Figure 18. Radar reflectivity at 0.5° elevation (scale at left) from the KMVX WSR-88D at 0054 UTC 27 August 2007, along with annotation for the storm motion of two supercells that merged prior to formation of the Northwood tornado (white arrows).

Supercell A, which produced its EF3 tornado with a path length of approximately 10 km between 0104 and 0116 UTC, was a classic "right-mover" in that it propagated almost due eastward at almost 20° to the right of the mean 0-6-km winds. In contrast, supercell B moved closer to the mean flow as its updraft developed less than 10 km south of supercell A, such that by 0115 UTC, the inflow notches and associated hook echoes of the two supercells were only about 9 km apart as the storms began to merge (Fig. 19). The two supercells continued their merger between 0119 and 0132 UTC, as evidenced by the 0.5° reflectivity imagery in Fig. 20. Finally, by 0136 UTC, the merger was complete and one supercell was evident in radar data near Northwood (Fig. 21). The numerical modeling simulations of Bluestein and Weisman (2000) and Jewett et al. (2002) generally suggested that cell interactions often negatively influence storm intensity. However, Lee et al. (2006) found that as many as 60% of the cell mergers in the 19 April 1996 Illinois outbreak resulted in an increase in cell rotation, similar to the Northwood tornado event.

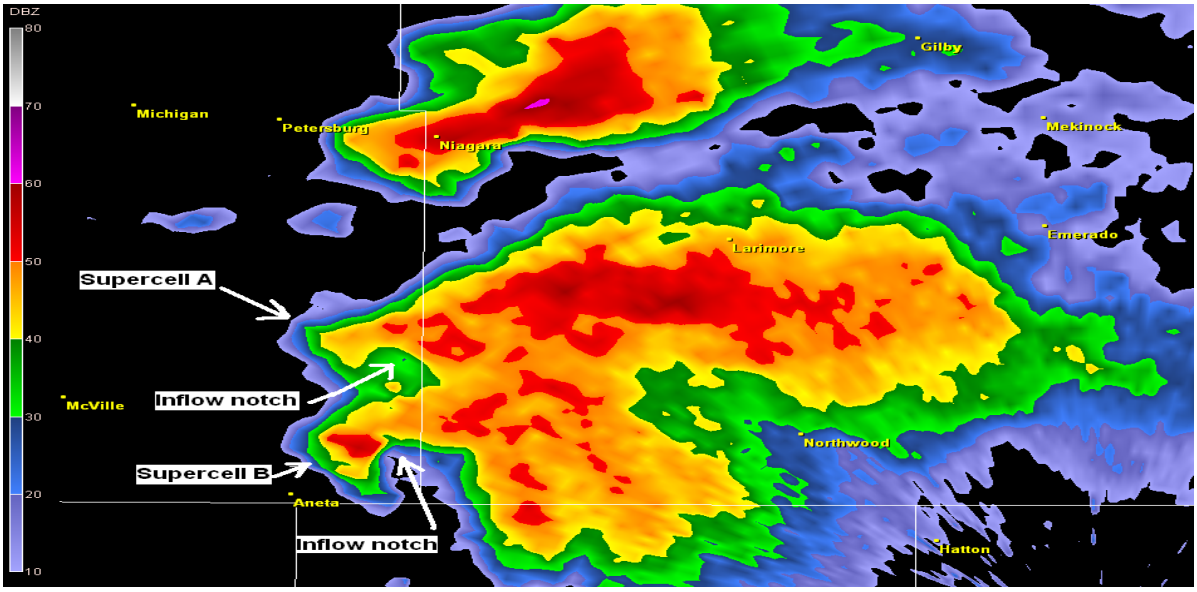

Figure 19. As in Fig. 18 (minus the white arrows annotating mesocyclone tracks), but at 0115 UTC 27 August 2007.

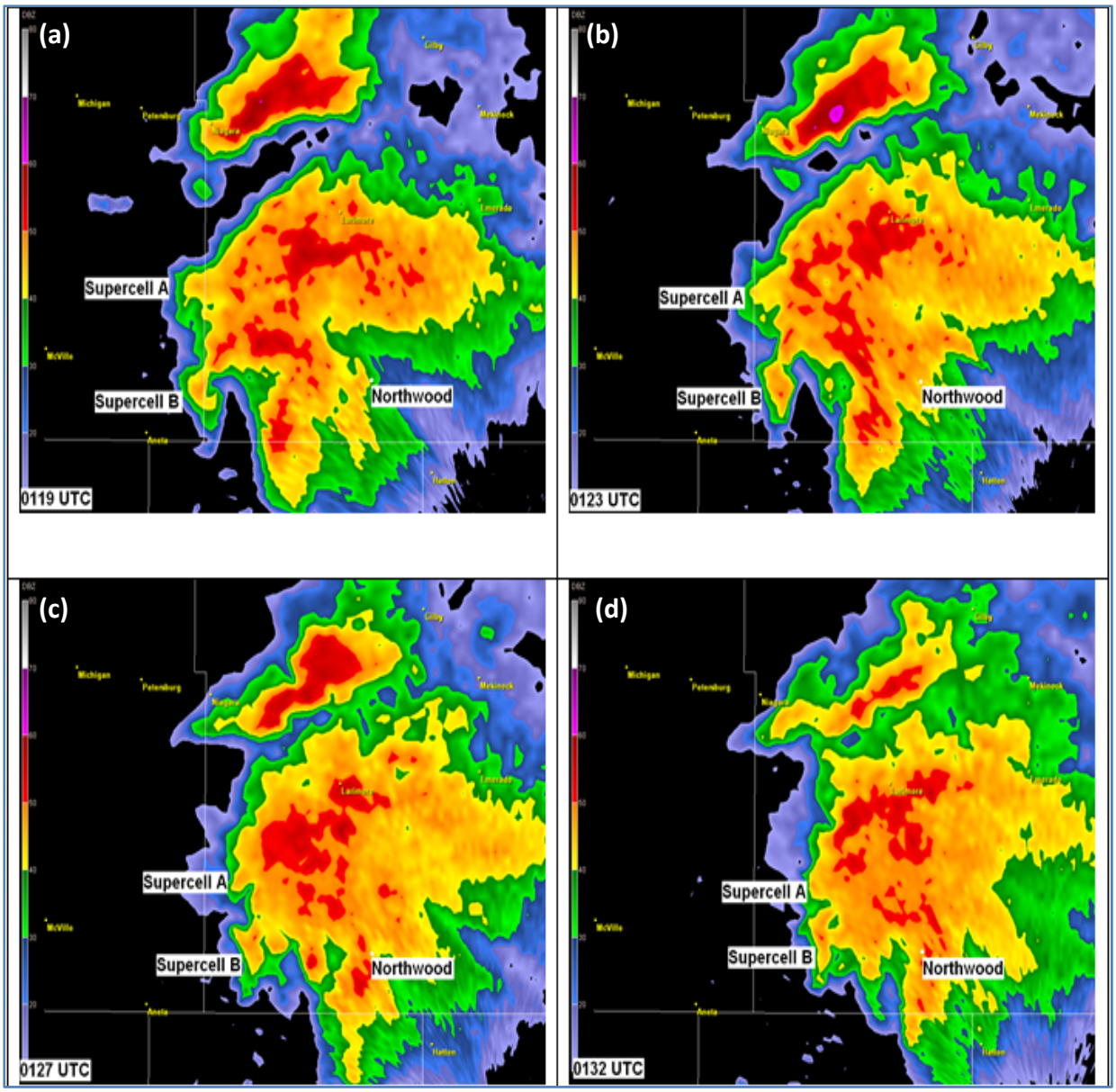

Figure 20. Radar reflectivity at 0.5° elevation (scale at left) from the KMVX WSR-88D showing merger of two supercells prior to the Northwood tornado on 27 August 2007 at a) 0119 UTC, b) 0123 UTC, c) 0127 UTC, and d) 0132 UTC.

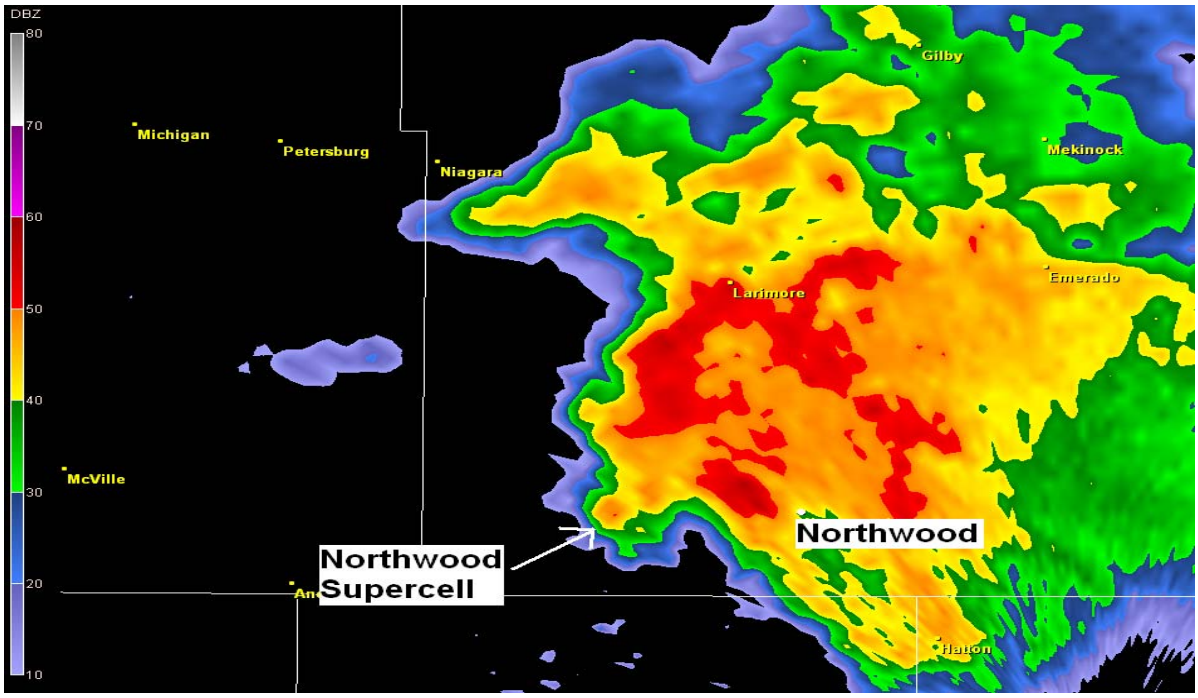

Figure 21. As in Fig. 18, but at 0115 UTC 27 August 2007.

A time series of 0.5° elevation angle velocity images from 0123 to 0157 UTC is shown in Fig. 22. The EF4 tornado affected the Northwood area between about 0142 and 0154 UTC. As shown in Fig. 22, during the period in which the supercell merger took place and before the Northwood tornado developed, an enhanced area of inbound velocity was detected near supercell A. The area of inbound velocity was shallow, only being observed up to the 0.9° elevation angle (not shown). It is hypothesized that this may have been outflow winds from supercell A, possibly from remnant rear- or forward-flank downdrafts as the low-level circulation from the first, EF3 tornado, occluded. The boundary resulting from this area of outflow winds was oriented from the southwest to northeast, and as the Northwood tornado moved through the town, the boundary appeared to interact with the strong GTG shear couplet on the northern side of the community.

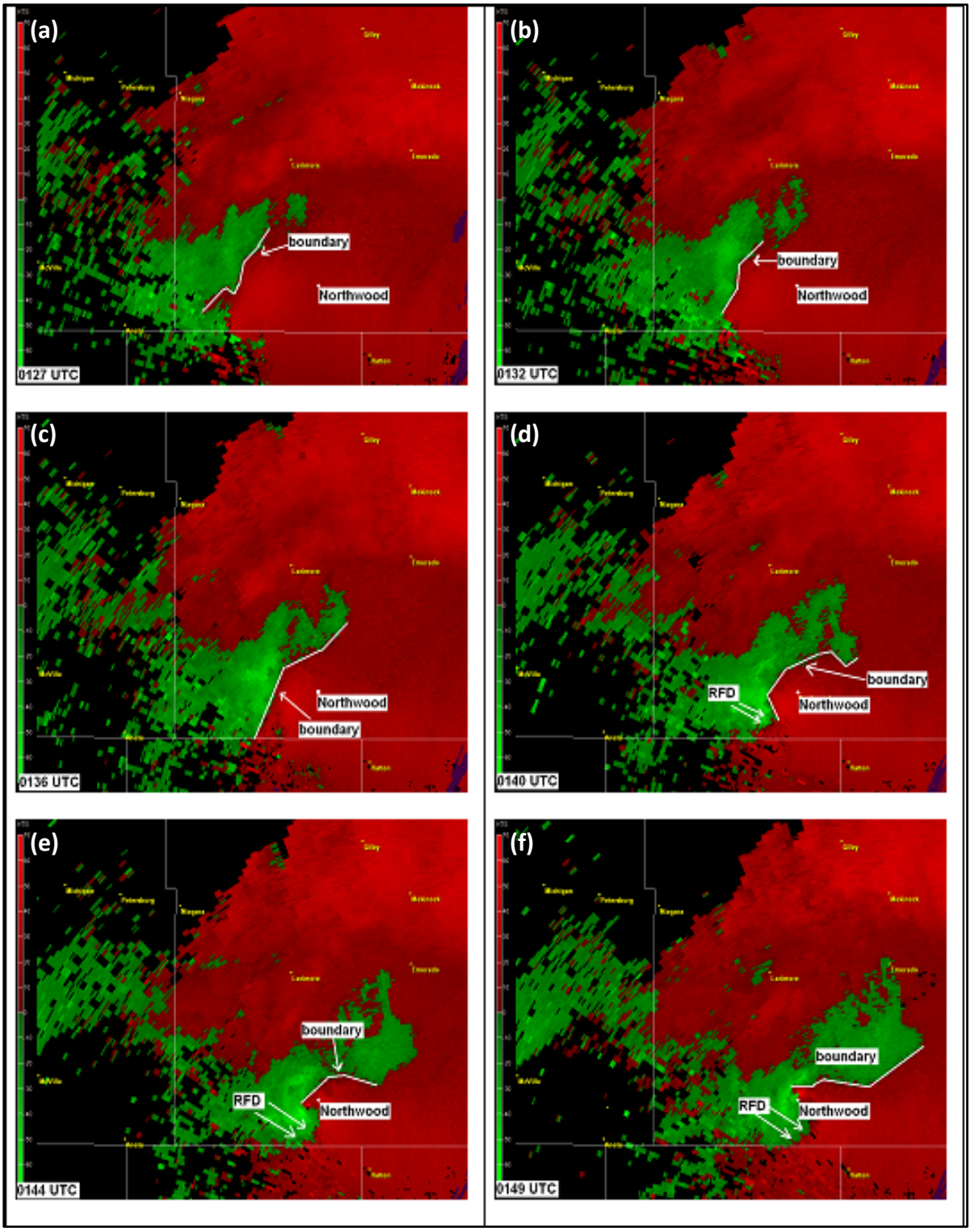

Figure 22. Radar velocity at 0.5° elevation from the KMVX WSR-88D showing boundary progression and rear-flank downdraft (RFD) evolution on 27 August 2007 at a) 0127 UTC, b) 0132 UTC, c) 0136 UTC, d) 0140 UTC, e) 0144 UTC, and f) 0149 UTC.

GTG shear, as determined using storm-relative velocity data at the 0.5° elevation angle, was maximized at almost 135 kt when the boundary interacted with the couplet (Fig. 23). That intersection was coincident with the location of the most severe damage, in an area where the official National Weather Service damage survey team found vehicles thrown a distance of 0.4 km (0.25 miles), and a mature corn field scoured to the soil. The damage survey team also found the tornado path turned sharply eastward beginning near the time of the intersection between the advancing boundary and the GTG shear couplet (Fig. 24). It is therefore hypothesized that this interaction may have tightened and intensified the tornadic circulation in the area of the most intense EF4 damage. In addition, the boundary continued surging southward after the tornado struck Northwood, so the relatively cool air behind it also may have eventually "undercut" the low-level inflow to the supercell, which may have contributed to the subsequent demise of the Northwood tornado.

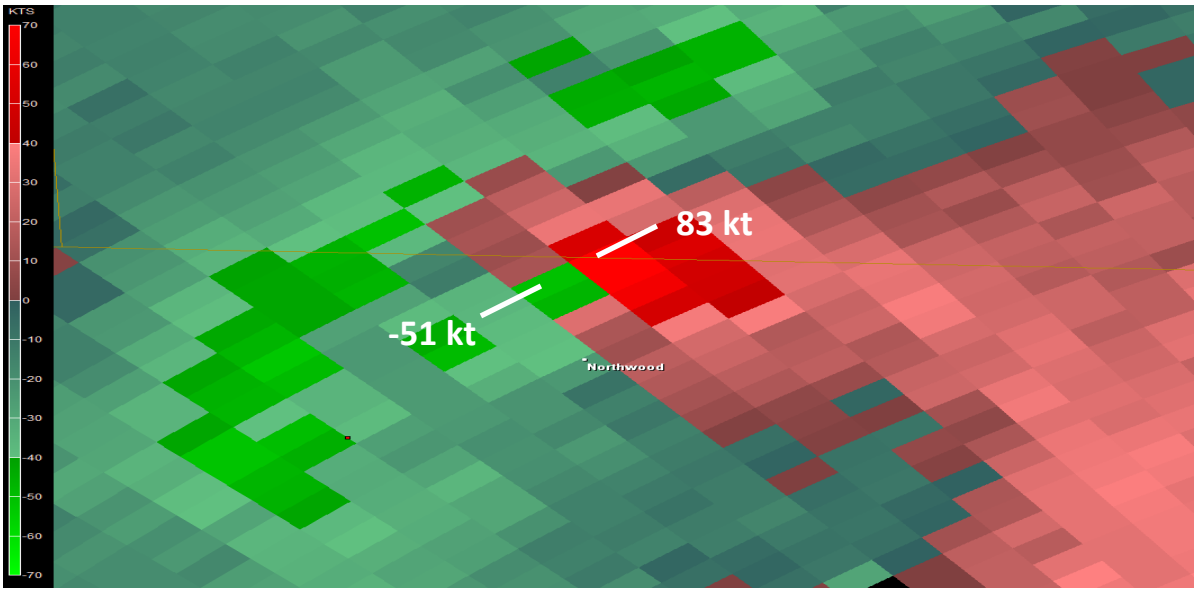

Figure 23. Radar storm-relative velocity at 0.5° elevation (scale at left) from the KMVX WSR-88D at 0149 UTC 27 August 2007, along with annotation of maximum inbound and outbound GTG storm-relative velocity values.

Figure 24. Tornado damage path (enclosed by red dashed lines) and approximate impact times (in CDT) through Northwood, North Dakota, as determined from official surveys and radar data.

The close proximity of the violent Northwood tornado to KMVX also allowed the radar to sample a tornadic debris signature (TDS; Bunkers and Baxter 2011). A TDS, or "debris ball," was evident in the 0.5° elevation angle reflectivity images between 0149 and 0159 UTC as the tornado affected the Northwood area and lofted debris into the area (Fig. 25). This caused particularly large scatterers to return up to 62 dBZ reflectivity echoes at the 0.5° elevation angle at 0153 UTC (Fig. 25c). This TDS was noted in real-time, and provided direct evidence that Northwood sustained a direct hit from the tornado. The highest dBZ values in reflectivity imagery also coincided directly with where the EF4 damage was observed. This would lend credence to the hypothesis that TDSs with higher dBZ values can be used as a proxy for the most significant damage within a tornado. TDSs, like this one, were also common during the 27 April

2011 tornado outbreak in the southeastern portion of the United States (Bunkers and Baxter 2011).

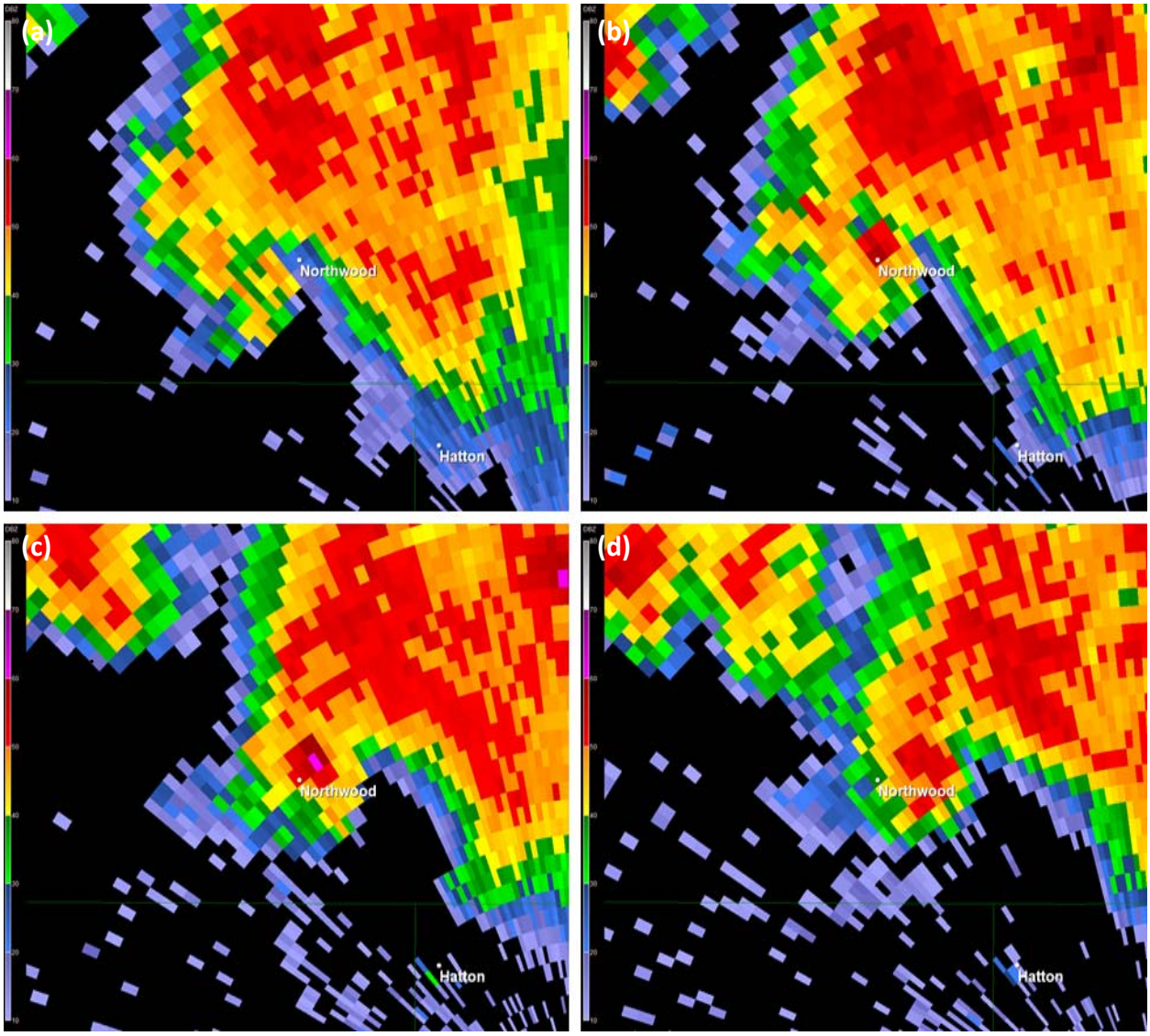

Figure 25. Radar reflectivity at 0.5° elevation from the KMVX WSR-88D on 27 August 2007 at a) 0144 UTC, b) 0149 UTC, c) 0153 UTC, and d) 0159 UTC.

The Northwood tornado was also investigated using the GR2Analyst radar interrogation software (www.grlevelx.com/gr2analyst). GR2Analyst allows a user to view radar reflectivity

cross sections using a defined dBZ value. For example, when looking at the 50 dBZ and higher reflectivity values from the Northwood tornado, debris can be seen at different levels in the 0149 and 0153 UTC images (Figs. 26 and 27). In addition, the debris can also be seen as it is being lifted into the tornado. Notice how the reflectivity increases into a cylindrical shape, likely a result of debris being lofted into the tornado. There was sheet metal and other large objects found over 1.6 km (1 mile) away from Northwood, and based on the images from GR2Analyst, the debris was likely lofted to a high level before descending again to the surface.

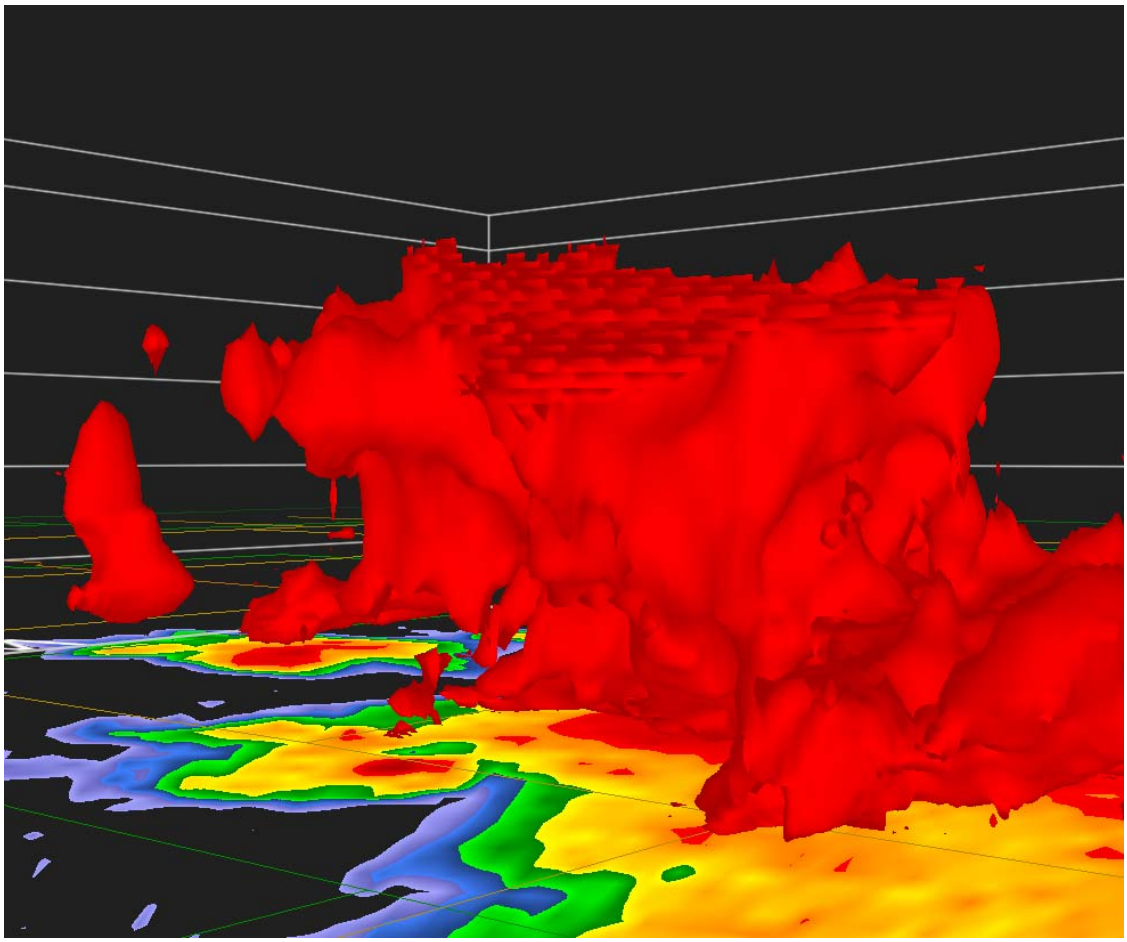

Figure 26. Three-dimensional image of reflectivity values greater than or equal to 50 dBZ from the KMVX WSR-88D and displayed using GR2Analyst at 0149 UTC 27 August 2007.

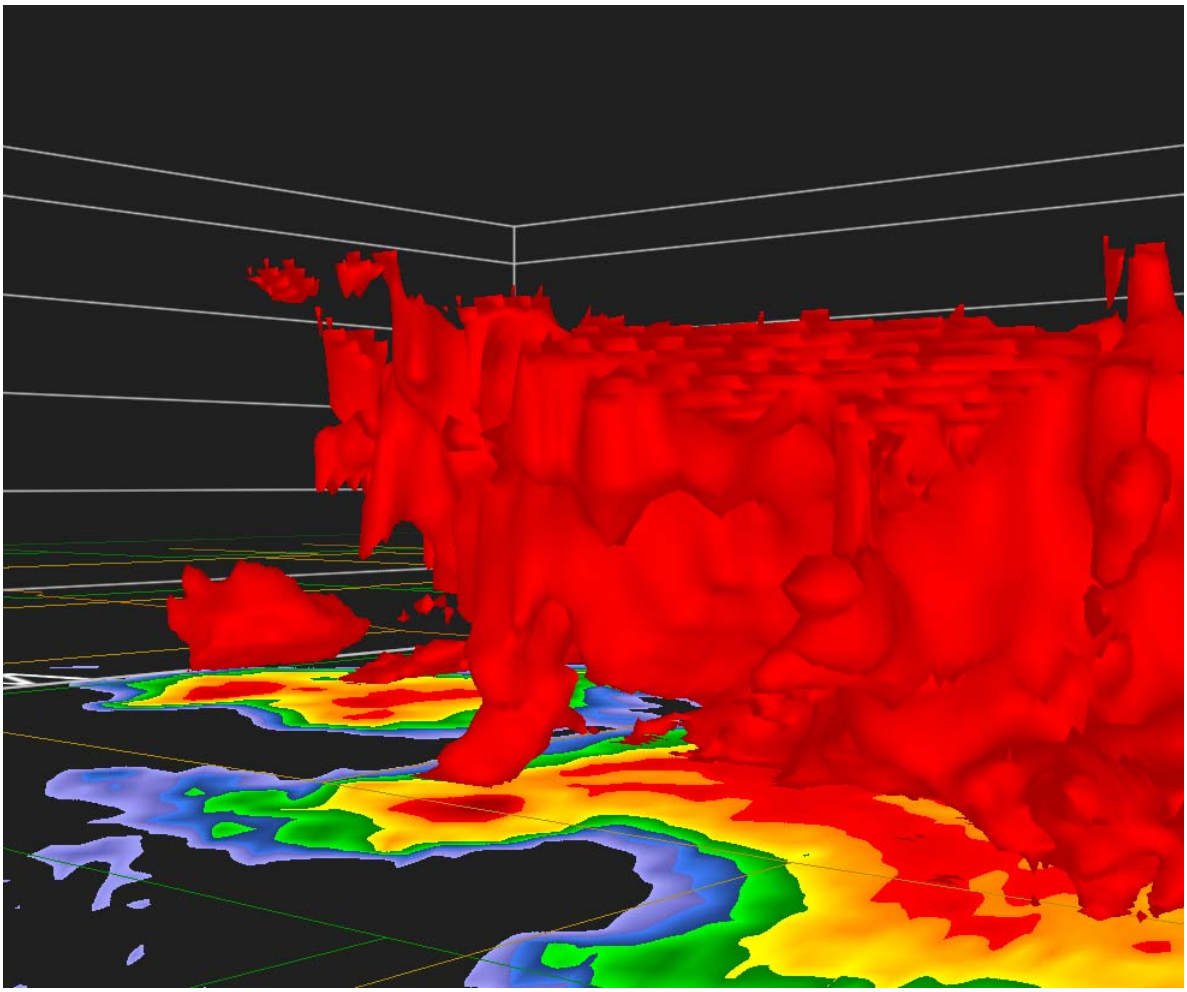

Figure 27. As in Fig. 26, but at 0153 UTC 27 August 2007.

4. Concluding Remarks

The 26 August 2007 northern Plains tornado outbreak was not easily anticipated. Decreased confidence in the forecast stage of the event was evident on multiple scales, from local significant tornado climatology and synoptic pattern recognition, to low confidence in convective initiation, and finally, the supporting nature of low-level shear without distinctly "backed" surface winds. It is not uncommon for certain tornado outbreaks to deviate from a classic textbook evolution, as demonstrated by the 3 May 1999 southern Plains outbreak,

wherein the supercells producing the most significant tornadoes appeared to occur in a setting with relatively large CAPE and "sufficient" but not extreme vertical wind shear (Thompson and Edwards 2000). The 26 August 2007 tornado outbreak also took place with large CAPE and significant, but not anomalous, wind shear. However, even though the background environment on 26 August 2007 resulted in several tornadoes, only one violent event occurred. It is strongly worth considering that the supercell which produced the EF4 tornado did so upon interaction with another cyclonically rotating supercell. The resulting radar signatures took place within close range to the operational WSR-88D and so this case is worthy of further investigation and similar-event comparisons.

The late-season 26 August 2007 tornado outbreak was considered to be a synoptically "uncommon" significant tornado-producer for the northern Plains. This strongly reaffirms the importance of an ingredients-based forecast methodology. The superimposed CAPE-shear setting fell within the range of previously observed strong and violent tornadoes. The presence of this environment was likely more important to the outbreak's occurrence than *how* the synoptic pattern arrived at the setting. Both climatology and pattern recognition certainly have their place in the tornado forecast process, but are no replacement for continual evaluation of the near-storm environment.

Acknowledgements

The authors are grateful for the thorough formal reviews of Brad Bramer, John Stoppkotte, Marc Singer, Keith Meier, and Jeff Manion, which substantially improved this study. The authors also thank Anthony Fischer for obtaining the WSR-88D VWP data and creating the hodographs used in section 2b.

REFERENCES

Bluestein, H. B., 1993: *Synoptic-Dynamic Meteorology in Midlatitudes. Vol. II: Observations and Theory of Weather Systems* . Oxford University Press, 594 pp.

Bluestein, H. B. and M. L. Weisman, 2000: The interaction of numerically simulated supercells initiated along lines. *Mon. Wea. Rev*., **128,** 3128–3149.

Bramer, B. J., D. T. Melde, E. J. Shimon, and G. R. Austin, 1998: An Examination of the Northern Plains Progressive Tornado Outbreak of 26 October 1996. Preprints, *19th Conf. on Severe Local Storms*, Minneapolis, MN, Amer. Meteor. Soc., 167–170.

Brooks, H. E., C. A. Doswell, and R. B. Wilhelmson, 1994: The Role of Midtrospheric Winds in the Evolution and Maintenance of Low-Level Mesocyclones. *Mon. Wea. Rev.*, **122**, 126–136.

Bunkers, M. J., B. A. Klimowski, J. W. Zeitler, R. L. Thompson, and M. L. Weisman, 2000: Predicting Supercell Motion Using a New Hodograph Technique. *Wea. Forecasting*, **15**, 61–79.

--., J. S. Johnson, L. J. Czepyha, J. M. Grzywacz, B. A. Klimowski, and M. R. Hjelmfelt, 2006b: An observational examination of long-lived supercells. Part II: Environmental conditions and forecasting. *Wea. Forecasting*, **21**, 689–714.

--.. and M. A. Baxter, 2011: Radar Tornadic Debris Signatures on 27 April 2011. *Electronic J. Operational Meteor*. **12** (7), 1-6.

Burgess D. W., M. A. Magsig, J. Wurman, D. Dowell, and Y. Richardson, 2002: Radar observations of the 3 May 1999 Oklahoma City tornado. *Wea. Forecasting*, **17**, 457-471.

Davies, J. M., and A. Fischer, 2009: Environmental characteristics associated with nighttime tornadoes. *NWA Electronic Journal of Operational Meteorology,* 2009-EJ3.

Dial, G. L., and J. P. Racy, 2004: Forecasting short term convective mode and evolution for severe storms initiated along synoptic boundaries. Preprints, *22nd Conf. on Severe Local Storms*, Hyannis, MA, Amer. Meteor. Soc., CD-ROM, 11A.2.

Garner, J., 2008: The Importance of a Well Mixed PBL in the Great Plains Severe Storm Environment. Presentation, *12th Annual High Plains AMS/NWA Conf.*, Hays, KS, available online.

Hart, J. A., and W. D. Korotky, 1991: The SHARP workstation user's manual—v1.50. A skewt/hodograph analysis and research program for the IBM and compatible PC. NOAA/NWS Forecast Office, Charleston, WV, 62 pp.

Jewett, B. F., R. B. Wilhelmson, and B. D. Lee, 2002: Numerical simulation of cell interaction. Preprints, *21st Conf. on Severe Local Storms*, San Antonio, TX, Amer. Meteor. Soc., 316–319.

Johns, R. H., J. C. Broyles, D. Eastlack, H. Guerrero, and K. Harding, 2000: The role of synoptic patterns and temperature and moisture distribution in determining the locations of strong and violent tornado episodes in the north central United States: A preliminary examination. *Preprints*, 20th Conf. Severe Local Storms, Orlando, FL, Amer. Meteor. Soc., 489-492.

Kellenbenz, D. J., T. J. Grafenauer, and J. M. Davies, 2007: The North Dakota tornadic supercells of 18 July 2004: Issues concerning high LCL heights and evapotranspiration. *Wea. Forecasting*, **22**:1200–1213.

Kerr, B. W. and G. L. Darkow, 1996: Storm-relative winds and helicity in the tornadic thunderstorm environment. *Wea. Forecasting*, **11**:489–505.

Lemon, L. R. and M. Umscheid, 2008: The Greensburg, Kansas, tornadic storm: A storm of extremes. Preprints, *24th Conf. on Severe Local Storms*, Savannah, GA, Amer. Meteor. Soc., P2.4.

Lee, B. D., B. F. Jewett, and R. W. Wilhelmson, 2006b: The 19 April 1996 Illinois Tornado Outbreak: Part II: Cell mergers and associated tornado incidence. *Wea. Forecasting*, **21**, 449-464.

Miller, D. J., 2006: Observations of low level thermodynamic and wind shear profiles on significant tornado days. Preprints, *23rd Conf. on Severe Local Storms*, St. Louis, MO, Amer. Meteor. Soc., 1206-1223.

Rasmussen, E. N., and D. O. Blanchard, 1998: A baseline climatology of sounding-derived supercell and tornado forecast parameters. *Wea.Forecasting*, **13**, 1148-1164.

--, 2003: Refined Supercell and Tornado Forecast Parameters. *Wea. Forecasting*, **18**, 530–535.

Rose, S. F., P. V. Hobbs, J.D. Locatelli, and M. T. Stoelinga, 2004: A 10-Yr Climatology Relating the Locations of Reported Tornadoes to the Quadrants of Upper-Level Jet Streaks. *Wea. Forecasting*, **19**, 301–309.

Schultz, C. J., 2009: Boundary Influences on the 7 July 2008 Tornado Event. *NWA Electronic Journal of Operational Meteorology*, 2009-EJ8.

Thompson, R. L., and R. Edwards, 2000: An Overview of Environmental Conditions and Forecast Implications of the 3 May 1999 Tornado Outbreak. *Wea. Forecasting*, **15**, 682-699.

--, --, J. A. Hart, K. L. Elmore, and P. Markowski, 2003: Close Proximity Soundings within Supercell Environments Obtained from the Rapid Update Cycle. *Wea. Forecasting*, **18**, 1243–1261.

--, and C. M. Mead, 2006: Tornado Failure Modes in Central and Southern Great Plains Severe Thunderstorm Episodes. Preprints, *23rd Conf. Severe Local Storms*, St. Louis, MO, Amer. Meteor. Soc, 3.2. [Available online at http://ams.confex.com/ams/pdfpapers/115239.pdf.]